

# A General Model-Based Approach to Two-Dimensional Infrared Correlation Spectroscopy Incorporating the Global Phase Angle

SHIN-ICHI MORITA, SARATCHANDRA SHANMUKH, YUKIHIRO OZAKI, and RICHARD A. DLUHY\*

University of Georgia, Department of Chemistry, Athens, Georgia 30602-2556 (S.-I.M., S.S., R.A.D.); and Kwansei Gakuin University, Department of Chemistry, School of Science and Technology 2-1 Gakuen, Sanda, Hyogo 669-1337, Japan (Y.O.)

We describe a theoretical framework for a model-based approach to two-dimensional correlation spectroscopy that is generally applicable to any arbitrary model function. The method is based on the correlation between spectral data and a set of model waveforms with a varying correlation index, the global phase angle  $\Theta$ . When experimental spectral intensity variations are expressed as sinusoidal, exponential, Lorentzian, or quadratic functions, the proposed approach allows us to estimate the quantitative values of the target parameters in those expressions. In addition, this method enables us to assess the sequential order in a series of bands undergoing non-identical intensity changes in a dynamic data set. We present both simulated and experimentally obtained data that illustrate that the deviations from linearity of the absorption band intensity waveforms are clearly detected and can be quantitatively estimated using quadratic functions.

Index Headings: Two-dimensional correlation infrared spectroscopy; Correlation spectroscopy; Global phase angle; Quantitative model; Sequential order.

## INTRODUCTION

The concept of a generalized approach to two-dimensional (2D) correlation spectroscopy was first proposed by Noda in 1993.<sup>1-4</sup> The theoretical framework of the generalized method directly correlates the experimentally measured variation in spectral intensities without the need to refer to an external model of intensity change. Based on this "model-free" approach, one can systematically analyze complex spectral intensity correlations for infrared (IR), Raman, ultraviolet-visible, or other types of optical signals.<sup>5-9</sup>

While the generalized 2D correlation analysis method is relatively straightforward to implement, interpretation of correlation spectra calculated using the model-free approach can be far from simple. This is because spectral intensity variations within a data set can have significantly different amplitudes, which give complicated synchronous and asynchronous 2D correlation maps. Also, in many cases, the positions and signs of the 2D correlation peaks can be accurately determined but the intensity values of the 2D correlation peaks have no physical meaning, due to the lack of a defined external reference standard. If an external intensity model could be successfully incorporated into the conventional 2D theoretical framework, it may be possible to discriminate against arbitrary signal amplitude changes that are not related to physically meaningful correlation peaks.

We have previously described modifications of the generalized 2D IR approach that make use of the fact that spectral intensity variations within a dynamic data set can be approximated by common mathematical functions.<sup>10,11</sup> In this

paper, we describe the theoretical framework for a model-based approach to 2D IR correlation spectroscopy that is generally applicable for any arbitrary model function. The calculation of the proposed 2D correlation spectrum visualizes the sequential order of signal intensity changes. Further, the sequential order can be discussed in a more quantitative manner when the experimental system is expressed by the sinusoidal, exponential, Lorentzian, or quadratic waveforms. These unique properties are not accessible from the conventional method given by Noda.<sup>1-4</sup> The simulation and application examples of the method are also demonstrated, in which the deviations from linearity of the absorption band intensity waveforms are clearly detected and quantitatively estimated using the quadratic function. The concepts proposed in this paper extend the applications of generalized 2D correlation spectroscopy and provide a new tool for analyzing perturbation-dependent spectroscopic phenomena.

## EXPERIMENTAL METHODS

2-Octadecyl-7,7,8,8-tetracyanoquinodimethane (octadecyl-TCNQ) was purchased from Kankoh-Shikiso Institute, Hayashibara Biochemical Laboratories, Inc., and used without further purification. Thin-layer chromatographic examinations revealed that they did not contain any other colored components. Water was prepared by passing city water through activated charcoal and reverse osmosis filters and then distillation. Finally, it was purified by an Ultrapure Water System Model CPW-101 (Advantec, Tokyo). The resistance of the finally prepared water was larger than 18.1 M $\Omega$  cm.

Langmuir-Blodgett (LB) films of octadecyl-TCNQ were fabricated using a Kyowa Kaimen Kagaku HBM-AP Langmuir trough with a Whilhelmy balance. Aliquots of a chloroform solution of octadecyl-TCNQ ( $1.0 \times 10^{-3}$  M) were spread onto a water subphase. After evaporation of the solvent, the monolayers were compressed at a constant rate of 20 cm<sup>2</sup>/min up to a surface pressure of 10 mN m<sup>-1</sup> (293 K). The  $\pi - A$  isotherm showed that the monolayers were solid condensed films at surface pressure of 10 mN m<sup>-1</sup>. At this pressure, the spread Langmuir film at the air-water interface was transferred onto a CaF<sub>2</sub> substrate by the vertical dipping method. The transfer ratio was found to be nearly unity throughout the experiments. The CaF<sub>2</sub> substrates were cleaned by ultrasonification in acetone, chloroform, and acetone, then in distilled water, and then by a homemade UV-ozone cleaner.

Infrared spectra were measured at a 4 cm<sup>-1</sup> resolution with a Nicolet Magna-IR Spectrometer 550 with an MCT detector. To generate the spectra with a high signal-to-noise ratio, 256 interferograms were coadded. To measure temperature-dependent IR spectra, the CaF<sub>2</sub> substrates on which the LB films had been deposited were inserted into a sample holder with

Received 2 June 2006; accepted 21 August 2006.

\* Author to whom correspondence should be sent. E-mail: dluhy@chem.uga.edu

thermocouple and a metal heater. Temperature control was achieved using an Omron EST temperature controller. The calibration line for the temperature measurements were developed to measure temperature more accurately at the point where the IR beam passed.

## RESULTS AND DISCUSSION: DESCRIPTION OF MODEL-BASED TWO-DIMENSIONAL INFRARED CORRELATION SPECTROSCOPY USING GLOBAL PHASE ANGLES

**Definition of a Model-Based Two-Dimensional Infrared Correlation Spectrum.** The approach proposed in this paper is based on the theoretical framework given by Noda.<sup>1-4</sup> The model-based 2D IR correlation analysis begins with a set of dynamically varying spectra, which are analyzed as a function of variable  $t$ , i.e.,  $y(v, t)$ . The spectra  $y(v, t)$  are obtained as a function of variable  $t$  with a fixed interval  $T = T_F - T_I$ , in which  $T_I$  and  $T_F$ , respectively, correspond to the initial and final values. The parameter  $t$  is referred to as “time” for convenience, although the spectra can be measured as a function of many experimental variables, e.g., temperature, pressure, concentration, etc., including chronological time. The valuable  $v$  can be one of several proper spectral variables (e.g., wavenumber, wavelength, Raman shift, etc.). The spectra  $y(v, t)$  are then transformed to the dynamic spectra  $\tilde{y}(v, t)$ , which are defined as

$$\tilde{y}(v, t) = \begin{cases} y(v, t) - \bar{y}(v) & \text{for } T: -T/2 \leq t \leq T/2 \\ 0 & \text{otherwise} \end{cases} \quad (1)$$

where the spectrum  $\bar{y}(v)$  is named the reference spectrum. The time-averaged spectrum of  $y(v, t)$  is usually used as the reference spectrum  $\bar{y}(v)$ . Note that the parameter  $t$  is transformed as  $t' - (T_F + T_I)/2 \rightarrow t$ . The replacement of the parameter  $t$  may be effective in deriving Hilbert transforms of mathematically expressed model waveforms.

A model waveform  $x(t)$  may also be defined within the time regime  $T$ . Selection of a model waveform is not predetermined. That is, a particular model waveform may be either experimentally measured or mathematically expressed. Its dynamic component  $\tilde{x}(t)$  is given by

$$\tilde{x}(t) = \begin{cases} x(t) - \bar{x} & \text{for } T \\ 0 & \text{otherwise} \end{cases} \quad (2)$$

where (as above), the time-averaged value of  $x(t)$  is usually used as the reference value  $\bar{x}$ . The waveform  $z(t)$ , without the symbol tilde, is calculated using the Hilbert transform, given by

$$z(t) = \frac{1}{\pi} p.v. \int_{-\infty}^{\infty} \frac{\tilde{x}(t')}{t' - t} dt' \quad (3)$$

where the integral symbol  $p.v.$  denotes that the Cauchy principal value is taken.<sup>2,4</sup> The waveform  $z(t)$  is transformed to its dynamic component  $\tilde{z}(t)$  using Eq. 2.

A series of coherent waveforms  $\tilde{y}_m(\Theta, t)$  are defined between orthogonal waveforms  $\tilde{x}(t)$  and  $\tilde{z}(t)$ , given by

$$\tilde{y}_m(\Theta, t) = \cos(\Theta) \cdot \tilde{x}(t) + \sin(\Theta) \cdot \tilde{z}(t) \quad (4)$$

where the parameter  $\Theta$  is named the global phase angle. In this paper, the range of the global phase angle  $\Theta$  is considered as  $-90^\circ \leq \Theta \leq 90^\circ$ , while the  $180^\circ$  range can be extended to  $360^\circ$ . The concept of the global phase angle as a method for 2D

amplitude normalization as well as its application to experimental data was previously discussed by Morita et al.<sup>12,13</sup>

The general method for model-based 2D IR correlation analysis is founded on the correlation between spectral data  $\tilde{y}_m(v, t)$  and a series of model waveforms  $\tilde{y}_m(\Theta, t)$ , given by

$$\Phi(v, \Theta) = \frac{1}{T} \int_T \tilde{y}(v, t) \cdot \tilde{y}_m(\Theta, t) dt \quad (5)$$

**Properties of a Model-Based Two-Dimensional Infrared Correlation Spectrum.** Figure 1 shows a schematic representation of a global model-based 2D-IR correlation spectrum based on Eq. 5 showing several correlation peaks. The global model-based 2D IR correlation map illustrated in Fig. 1 is similar to previously published model-based 2D methods in which the calculated model parameter is plotted as a function of the spectral variable.<sup>10,11</sup> In Fig. 1, the  $\Theta$  value with the largest absolute value of  $\Phi$  is obtained when the  $\Theta$ -dependent model waveform  $\tilde{y}_m(\Theta, t)$  or  $-\tilde{y}_m(\Theta, t)$  matches closest to the waveform of the spectral data  $\tilde{y}(v, t)$ . The  $\Theta$  value at that point is defined as a new parameter, named the effective global phase angle  $\Theta_E(v)$ .

In general, the effective global phase angle  $\Theta_E(v)$  serves as a versatile correlation index with the ability to determine the sequential order of the variation in signal intensity, although the index  $\Theta_E(v)$  itself does not have any concrete physical meaning such as a fixed time delay in sinusoidal systems. Here we recognize that the concept “sequential order” is invariant to signal amplitudes, and it is only related to signal waveforms. The following information about the temporal nature of the correlation peaks can be obtained from the  $\Theta_E(v)$  index:

If  $\Theta_E(v) > 0^\circ$ , the change at  $v$  occurs *before* that in the model.

If  $\Theta_E(v) = 0^\circ$ , the change occurs *simultaneously*, compared with that in the model.

If  $\Theta_E(v) < 0^\circ$ , the change at  $v$  occurs *after* that in the model.

These conventions regarding the sequential order of the effective global phase angle are based on the inherent properties of generalized 2D correlation spectroscopy<sup>1,3,4</sup> and have been previously demonstrated using other model-based approaches.<sup>10,11</sup>

Under certain circumstances, the effective global phase angle  $\Theta_E(v)$  may also be used as a quantitative index to estimate the target parameter of a model waveform. Typical cases are summarized in Table I. The waveforms in this table (i.e., sinusoidal, exponential, Lorentzian, and quadratic) are

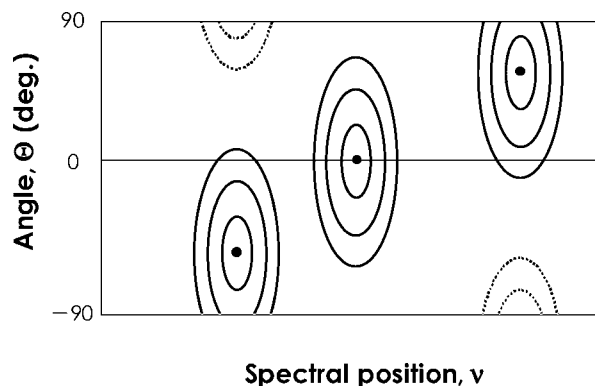


FIG. 1. A schematic illustration of a model-based 2D IR spectrum. The dashed lines are used for negative correlation peaks.

frequently utilized as representations of experimentally measured spectral intensity variations in dynamic data sets. For instance, sinusoidal functions can be used to model the spectral response of samples subject to a repetitive external perturbation,<sup>14</sup> and exponential response curves are commonly observed in the chemical kinetics monitored by spectroscopy.<sup>15</sup> Also, a time-domain Lorentzian type waveform can be a proper model response function for chromatographs equipped with spectroscopic detection.<sup>16</sup> A quadratic function may be utilized to express a deviation from a linear intensity spectral change (*vide infra*).

As for the sinusoidal system in Table I, the parameter  $A$  determines the amplitude of the sinusoidal intensity change, and  $\beta$  is the phase of the sinusoidal function with the frequency  $\Omega$ ; the exponential decaying waveform is expressed by the parameters  $A$  and  $k$ , which respectively correspond to the  $y(t)$  or  $x(t)$  value at  $t = 0$  and the rate constant of the exponentially decaying process; the Lorentzian function is given by the parameters  $A$ ,  $w$ , and  $\tau$ , corresponding respectively to the height, width, and position of the Lorentzian type distribution; the quadratic function is expressed by the parameters  $k_2$  and  $k_1$  and the ratio is defined as the target parameter  $K_{21}$ .

**Simulation Examples of Model-Based Two-Dimensional Infrared Correlation Spectroscopy.** The usefulness of this model-based approach to 2D correlation analysis is illustrated by simulating the concentration-dependent IR spectra of three different molecules in liquid solution. Here, the concentration  $c$  is used as the perturbation. Figure 2a shows a schematic diagram of the experimental system. We assume that a transparent liquid cell contains a solution of the molecules P, Q, and R, each at an initial concentration  $C_1$ . For the purposes of this example, we assume that over time the solvent evaporates, increasing the concentration of the solute molecules. The evaporation process is monitored by IR transmission spectroscopy from initial  $C_1 = 0.01$  to final concentration  $C_F = 0.02$  (101 spectra with constant intervals of concentration).

Figure 2b shows the type of absorbance band intensity response that may be expected in this system. In most cases, the changes in the peak heights of absorption bands with concentration will obey a classic Beer–Lambert relationship, that is, the absorbance response will be linear as a function of concentration (curve A). However, an increased molecular concentration can also result in a nonlinear Beer–Lambert relationship due to, e.g., molecular aggregation<sup>17</sup> as exemplified by curve B. By using a simple linear Beer–Lambert relationship to simulate the change in concentration, we can test whether the proposed 2D IR correlation method can detect deviations from this model waveform. We expect that a positive deviation from Beer’s Law (e.g., curve B) will be detected as a larger value of the effective global phase angle than that of the linear model, i.e.,  $\Theta_E(\nu) > 0^\circ$ .

Figure 3a shows the simulated concentration-dependent IR spectra of the liquid solution used in this analysis. The absorption bands at 1550, 1480, and 1430 are named bands P, Q, and R, respectively. The simulated IR spectra in Fig. 3a were produced by the equation

$$y(\nu, c) = \frac{-5000c^2 + 200c}{(\nu - 1550)^2 + 25} + \frac{100c}{(\nu - 1480)^2 + 25} + \frac{-2400c^2 + 120c}{(\nu - 1430)^2 + 25} \quad (6)$$

The three terms on the right side of Eq. 6 correspond to bands P, Q, and R, respectively. Each band shape was simulated by a Lorentzian function (the denominator of the each term), while the concentration-dependent intensity change for each band was simulated by a second-degree polynomial function (the numerator of the each term).

Figure 3b shows the corresponding 2D IR correlation spectrum where the linear Beer–Lambert relationship is used as the model (i.e.,  $x(c) = \bar{x}(c) = 10c$ ). The averaged spectrum  $\bar{y}(\nu, c)$  is used as the reference spectrum in the calculation of dynamic spectra in this model. The effective global phase angle values corresponding to the bands  $\nu = 1550$ , 1480, and 1430 are calculated as  $\Theta_E(1550) = 8.86^\circ$ ,  $\Theta_E(1480) = 0.04^\circ$ , and  $\Theta_E(1430) = 4.42^\circ$ , respectively.

Figure 3b illustrates the ability of the effective global phase angle index  $\Theta_E(\nu)$  to determine the sequential order of the signal intensity changes in a series of bands undergoing non-identical intensity changes in a dynamic data set. In the current example:

- (1) The signal intensity change  $y(1550, c)$  occurs at  $\Theta_E = 8.86^\circ$ , indicating that the change occurs *before* that in the Beer’s Law model.
- (2) The change  $y(1480, c)$  occurs at  $\Theta_E = 0.04^\circ$ , which indicates *simultaneous* behavior with the model.
- (3) The change  $y(1430, c)$  occurs at  $\Theta_E = 4.42^\circ$ , indicating that the change occurs *before* that in the model.

The quantitative nature of this approach may be illustrated by the following example. Taking the saturation phenomena into account, the spectral changes in the experimental system can be expressed by the quadratic function, given by

$$y(\nu, c) = \begin{cases} k_2(\nu)c^2 + k_1(\nu)c + k_0(\nu) & \text{for } C_1 \leq c \leq C_F \\ 0 & \text{otherwise} \end{cases} \quad (7)$$

As shown in Table I, the  $\Theta_E(\nu)$  index for each peak in Fig. 3 can be related to the parameter  $K_{21}(\nu) \equiv k_2(\nu)/k_1(\nu)$  of the quadratic function, given by

$$K_{21}(\nu) = \frac{-2\pi \tan \Theta_E(\nu)}{2\pi \tan \Theta_E(\nu)(C_F + C_1) + (C_F - C_1)} \quad (8)$$

Using the above equation, the  $K_{21}$  values for the three correlation peaks are calculated as  $K_{21}(1550) = -24.9$ ,  $K_{21}(1480) = -0.5$ , and  $K_{21}(1430) = -19.8$ , respectively. These values agree well with the corresponding values for bands P, Q, and R that were used in the simulation, i.e.,  $K_{21} = -25.0, \pm 0.0$ , and  $-20.0$ .

**Application of Model-Based Two-Dimensional Infrared Correlation Spectroscopy to Temperature-Dependent Reorganization in Thin Films.** The pre-melting behavior of an eleven-layered Langmuir–Blodgett (LB) film of 2-octadecyl-7,7,8,8-tetracyanoquinodimethane (octadecyl-TCNQ)<sup>18–20</sup> was analyzed using the model-based 2D IR correlation spectroscopy methods presented here. Figure 4 shows the temperature-dependent IR transmission spectra of an LB film of octadecyl-TCNQ acquired as the sample temperature was increased between 70 and 110 °C with increments of 2 °C (21 spectra). Here, the temperature  $t$  is used as the sample perturbation. The two major bands at 2918 and 2848  $\text{cm}^{-1}$  are due to the  $\text{CH}_2$  anti-symmetric and symmetric stretching modes, respectively.<sup>18,20</sup>

For hydrocarbon assemblies on solid surfaces, the  $\text{CH}_2$  anti-symmetric and symmetric bands give maximum peak intensi-

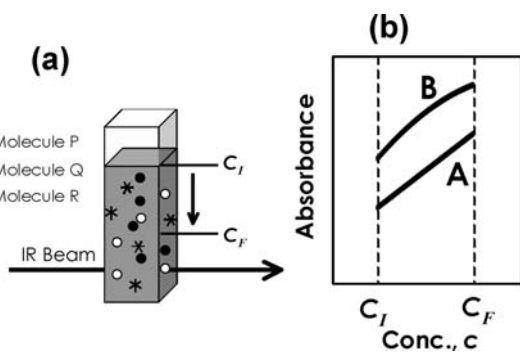
**TABLE I.** The waveforms (i.e., sinusoidal, exponential, Lorentzian, and quadratic) frequently utilized as representations of experimentally measured spectral intensity variations in dynamic data sets.

System $y(t)$	Model $x(t)$	Relationship of target parameter to $\Theta_E$
$A \sin(\Omega t + \beta)$ $-\infty \leq t \leq \infty$ $\bar{y} = 0$	$A' \sin(\Omega t + \beta')$ $-\infty \leq t \leq \infty$ $\bar{x} = 0$	$\beta = \beta' + \Theta_E$
$A \exp(-kt)$ $0 \leq t \leq \infty$ $\bar{y} = 0$	$A' \exp(-k't)$ $0 \leq t \leq \infty$ $\bar{x} = 0$	$k = k' \exp(\pi \tan \Theta_E)$
$A w^2$ $w^2 + (t - \tau)^2$ $-\infty \leq t \leq \infty$ $\bar{y} = 0$	$A' w'^2$ $w'^2 + (t - \tau')^2$ $-\infty \leq t \leq \infty$ $\bar{x} = 0$	$\tau = \tau' - 2w' \tan \Theta_E$ if $w \approx w'$
$k_2 t^2 + k_1 t + k_0$	$k'_1 t + k'_0$	$K_{21} = \frac{k_2}{k_1}$
$T_1 \leq t \leq T_F$	$T_1 \leq t \leq T_F$	$K_{21} = \frac{-2\pi \tan \Theta_E}{2\pi \tan \Theta_E (T_F + T_1) + (T_F - T_1)}$
$\bar{y}$ : $t$ -averaged	$\bar{x}$ : $t$ -averaged	

ties when a hydrocarbon chain is in the all-*trans* conformation with its long axis perpendicular to the substrate surface.<sup>21,22</sup> In the current experimental configuration, the electric vector incident of the IR light was set parallel to a substrate surface, in which only the component of a transition moment parallel to the substrate surface is observed. In addition, the direction of the long axis of the all-*trans* chain and the transition moments of these two modes are perpendicular to one another.<sup>23</sup>

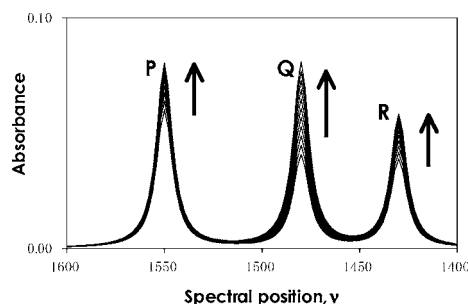
Figure 4 shows that the peak intensities of both bands decrease during the heating process between 70 and 110 °C. The intensity decrease in these bands indicates that the hydrocarbon chain gradually changes into a more disordered state due to its micro-Brownian motion, while the macroscopic order in the LB film is still retained due to the attraction forces between TCNQ chromophore planes. Note that at these temperatures, octadecyl-TCNQ is still in a mostly ordered phase since the order-disorder transition for this molecule occurs at 118 °C.<sup>20</sup>

Figure 5 shows the 2D correlation spectrum, in which the linear function  $x(t) = -0.0005t + 0.085$  is used as a simple model waveform. The effective global phase angle values for the two bands are estimated as  $\Theta_E(2918) = 5.62^\circ$  and  $\Theta_E(2848) = -6.23^\circ$ , indicating that (1) the change at 2918  $\text{cm}^{-1}$  occurs *before* that in the model, and (2) the change at 2848  $\text{cm}^{-1}$



**FIG. 2.** (a) A schematic representation of the simulated experimental system. The evaporation process is monitored by the IR transmission method from  $C_I = 0.01$  to  $C_F = 0.02$  so that each spectrum is measured as a function of concentration. (b) Typical intensity responses expected in the system.

(a)



(b)

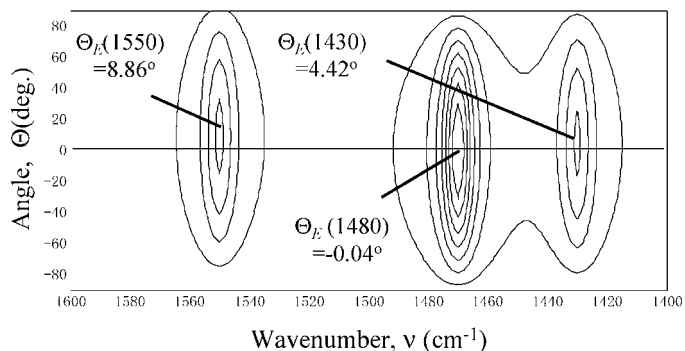


**FIG. 3.** (a) Simulated concentration-dependent IR transmission spectra of a liquid solution consisting of molecules P, Q, and R. Among the 101 spectra, only 11 spectra are shown. (b) The corresponding model-dependent 2D IR correlation spectrum based on the effective global phase angle calculated for the simulated IR data in (a). The Beer-Lambert law was used as the model waveform in these calculations.

occurs *after* that in the model. The differences in the global phase angle values can be interpreted as the detection of the change in the orientation of the alkyl chain from the ordered state to the isotropic one.

This experimental system also allows us to estimate the

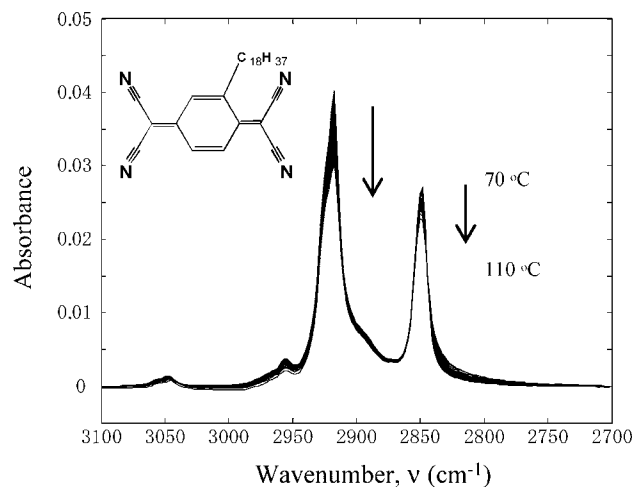


**FIG. 4.** Temperature-dependent IR transmission spectra of the eleven-layer LB film of octadecyl-TCNQ from 70 to 110 °C with increments of 2 °C (21 spectra).

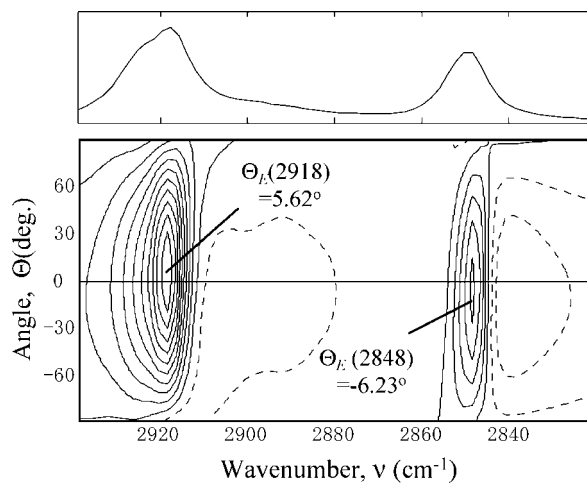


FIG. 5. The 2D correlation spectrum based on the effective global phase angle calculated for the temperature-dependent IR spectra shown in Fig. 4. A simple linear function was used as the model waveform.

deviations from the linear intensity change quantitatively using the quadratic function. The quadratic function is given as

$$y(v, t) = \begin{cases} k_2(v)t^2 + k_1(v)t + k_0(v) & \text{for } T_I \leq t \leq T_F \\ 0 & \text{otherwise} \end{cases} \quad (9)$$

Here we recognize that  $T_I$  and  $T_F$ , respectively, indicate the initial and final values of the temperature range observed (this case,  $T_I = 70$  °C and  $T_F = 110$  °C.) As shown in Table I, the target parameter  $K_{21}(v)$  can be estimated by

$$K_{21}(v) = \frac{-2\pi \tan \Theta_E(v)}{2\pi \tan \Theta_E(v)(T_F + T_I) + (T_F - T_I)} \quad (10)$$

The  $K_{21}$  values are respectively estimated as  $K_{21}(2918) = -0.0041$  and  $K_{21}(2848) = -0.0082$ . Using these  $K_{21}$  values, the intensity profiles can be reconstructed as shown in Fig. 6, and the reconstructed curves respectively agree well with the original experimentally obtained data.

## CONCLUSION

A model-based approach to 2D IR correlation spectroscopy is proposed that is generally applicable to any arbitrary model waveform. The advantages of a model-based approach lie in its ability to visualize the sequential order of a signal intensity change in a dynamic data set, and its ability to quantitatively estimate the sequential order using a specific model waveform (e.g., sinusoidal, exponential, Lorentzian, or quadratic). The usefulness of this model-based approach is demonstrated by simulating the concentration-dependent IR spectra of three different molecules in liquid solution, in which the deviations from the linear intensity change are clearly detected. The proposed analytical method was applied to the temperature-dependent IR transmission spectra of an octadecyl-TCNQ LB film. A linear intensity change was used as the model waveform, and the 2D correlation peaks due to the  $\text{CH}_2$  anti-symmetric and  $\text{CH}_2$  symmetric stretching modes were shown to produce positive and negative values of the effective global phase angle, respectively. The different phase angle values for the two bands indicated that the intensity change in the  $\text{CH}_2$  anti-symmetric band occurred prior to the linear intensity

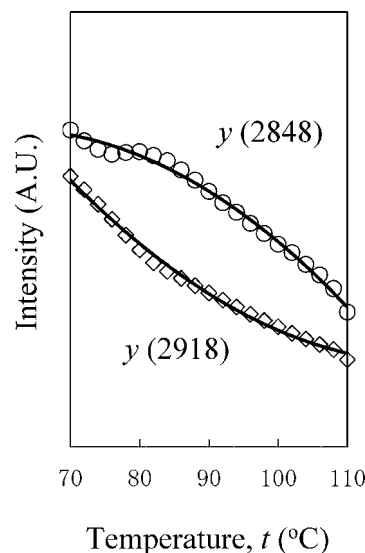


FIG. 6. The signal intensity profiles reconstructed based on the  $K_{21}$  values estimated through the 2D correlation analysis (solid lines). The original data experimentally obtained are indicated by open circles and squares. The longitude scale of the each profile is arbitrarily adjusted for comparison purpose.

change in the model while the change in the  $\text{CH}_2$  symmetric band occurred after the model waveform. The deviations from the linear intensity change were quantitatively estimated assuming a quadratic function. In this example, the reconstructed quadratic waveforms agree with the original experimentally obtained data, providing a confirmation of the validity of the method.

There are many additional aspects of this model-based approach to 2D correlation analysis that may be examined, including (1) resolution enhancement effects, (2) the effect that band parameter changes such as peak shifts, overlapping, and broadening features have on the 2D maps, (3) the direct comparison of effective global phase angle values at different spectral positions, and (4) the use of other analytic functions for quantitative estimation of the target parameters. Our laboratory is currently investigating these questions.

## ACKNOWLEDGMENTS

The work described here was supported by the U.S. Public Health Service through National Institutes of Health grant EB001956 (R.A.D.).

1. I. Noda, *Appl. Spectrosc.* **47**, 1329 (1993).
2. I. Noda, *Appl. Spectrosc.* **54**, 994 (2000).
3. I. Noda, A. E. Dowrey, C. Marcott, G. M. Story, and Y. Ozaki, *Appl. Spectrosc.* **54**, 236A (2000).
4. I. Noda and Y. Ozaki, *Two-Dimensional Correlation Spectroscopy - Applications in Vibrational and Optical Spectroscopy* (John Wiley and Sons, Chichester, 2004).
5. V. G. Gregoriou, J. L. Chao, H. Toriumi, and R. A. Palmer, *Chem. Phys. Lett.* **179**, 491 (1991).
6. M. Mueller, R. Buchet, and U. P. Fringeli, *J. Phys. Chem.* **100**, 10810 (1996).
7. I. Noda, Y. L. Liu, and Y. Ozaki, *J. Phys. Chem.* **100**, 8665 (1996).
8. Y. Z. Ren, M. Shimoyama, T. Ninomiya, K. Matsukawa, H. Inoue, I. Noda, and Y. Ozaki, *J. Phys. Chem. B* **103**, 6475 (1999).
9. T. C. Holmes, S. de Lacalle, X. Su, G. Liu, A. Rich, and S. Zhang, *Proc. Natl. Acad. Sci. U.S.A.* **97**, 6728 (2000).
10. D. L. Elmore and R. A. Dluhy, *J. Phys. Chem. B* **105**, 11377 (2001).
11. S. Shanmukh and R. A. Dluhy, *J. Phys. Chem. A* **108**, 5625 (2004).
12. S. Morita, Y. Ozaki, and I. Noda, *Appl. Spectrosc.* **55**, 1618 (2001).

13. S. Morita, Y. Ozaki, and I. Noda, *Appl. Spectrosc.* **55**, 1622 (2001).
14. I. Noda, *Appl. Spectrosc.* **44**, 550 (1990).
15. K. Masutani, in *Handbook of Vibrational Spectroscopy*, J. M. Chalmers and P. R. Griffiths, Eds. (John Wiley and Sons, Chichester, 2002), pp. 655–665.
16. P. R. Griffiths and J. A. de Haseth, *Fourier Transform Infrared Spectrometry* (John Wiley and Sons, New York, 1986).
17. J. Louch and J. D. Ingle, Jr., *Anal. Chem.* **60**, 2537 (1988).
18. Y. Wang, K. Nichogi, S. Terashita, K. Iriyama, and Y. Ozaki, *J. Phys. Chem.* **100**, 368 (1996).
19. Y. Wang, K. Nichogi, K. Iriyama, and Y. Ozaki, *J. Phys. Chem.* **100**, 374 (1996).
20. S. Morita, K. Nichogi, and Y. Ozaki, *J. Phys. Chem. B* **108**, 7871 (2004).
21. R. G. Snyder, H. L. Strauss, and C. A. Elliger, *J. Phys. Chem.* **86**, 5145 (1982).
22. D. L. Allara, A. Baca, and C. A. Pryde, *Macromolecules* **11**, 1215 (1978).
23. C. Naselli, J. F. Rabolt, and J. D. Swalen, *J. Chem. Phys.* **82**, 2136 (1985).